

## REFERENCES

- Allan, R. S., and Mason, S. G. (1961). Transactions of the Faraday Society, 57, 2027.
- Barnes, H. A., Hutton, J. F., and K., Walters, F. R. S. (1989). An introduction to rheology. 1st ed. Amsterdam: Elsevier Science Publishers B. V.
- Bentley, B. J., and Leal, L. G., (1986). A computer-controlled four-roll mill for investigation of particle and drop dynamics in two-dimensional linear shear flows. Journal of Fluid Mechanics, 167, 219-240.
- Bentley, B. J., and Leal, L. G. (1986). An experimental investigation of drop deformation and break-up in steady, two dimensional linear flow. Journal of Fluid Mechanics, 167, 241.
- Bourry, D. and Favis, B. D. (1998). Morphology development in a polyethylene/polystyrene binary blend during twin-screw extrusion. Polymer, 39(10), 1851-1856.
- Brandrup, J., and Immergut, E. H. (Eds.) (1989). Polymer handbook, Vol.2, (441-434). New York: John Wiley & Son.
- Chesters, A. K. (1991). The modeling of coalescence processes in fluid-liquid dispersions: A review of current understanding. Trans. Ind. Chem. Eng., 69A, 259-270.
- De Bruijn, R. A. (1989). Deformation and breakup of drops in simple shear flow. Ph.D Thesis, Eindhoven University of Technology, Eindhoven, The Netherlands.
- Dealy, J. M. and Wissbrun, K. F. (1990). Melt rheology and its role in plastics processing: Theory and applications. New York: Van Nostrand Reinhold.
- Elmendorp, J. J., and Maalcke, R. J. (1986). A study on polymer blending microrheology: Part I. Polymer Engineering and Science, 25, 1041-1047.

- Elmendorp, J. J., and van der Vegt, A. K. (1986). A study on polymer blending microrheology: Part IV. Polymer Engineering and Science, 26, 1332-1338.
- Favis, B. D., and Chalifoux, J. P. (1987). The effect of viscosity ratio on the morphology of polypropylene/polycarbonate blends during processing. Polymer Engineering and Science, 27(20), 1591-1600.
- Fortelny, I., and Zivny, A. (1998). Film drainage between droplets during their coalescence in quiescent polymer blends. Polymer, 12, 2669-2675.
- Flumerfelt, R. W. (1972). Drop breakup in simple shear fields of viscoelastic fluids. Ind Eng Chem Fundam, 11, 312-318.
- Gauthier, F., Goldsmith, H. L., and Mason, S. G. (1971). Particle motions in non-Newtonian media II: Poiseuille flow. Transactions of the Society of Rheology, 15, 297-330.
- Grace, H. P. (1982). Dispersion phenomena in high viscosity immiscible fluid systems and application of static mixers as dispersion devices in such systems. Chem Eng Commun, 14, 225-277.
- Levitt, L., Macosko, C. W., and Pearson S. D. (1996). Influence of normal stress difference on polymer drop deformation. Polymer Engineering and Science, 36(12), 1647-1655.
- Mighri, F., Aji, A., and Carreau, P. J. (1997). Influence of elastic properties on drop deformation in elongational flow. Journal of Rheology, 41, 1183-1201.
- Mighri, F., Aji, A., and Carreau, P. J. (1998). Influence of elastic properties on drop deformation and breakup in shear flow. Journal of Rheology, 42, 1477-1490.
- Milliken, W. J., and Leal, L.G. (1991). Deformation and breakup of viscoelastic drops in planar extensional flows. Journal of Non-Newtonian Fluid Mechanics, 40, 355-379.

- Minale, M., Mewis, J., and Moldenaers, P. (1998). Study of the morphological hysteresis in immiscible polymer blends. AICHE Journal, 44, 943-950.
- Park, D. W., and Roe, R. J. (1991). Macromolecules, 24, 5324.
- Roland, C. M., and Böhm, G. G. A. (1984). Journal of Polymer Science, Polymer Physics, 22, 79.
- Rumscheidt, F. D., and Mason, S. G. (1961). Particle motions in sheared suspension: Deformation and burst of fluid drops in shear and hyperbolic flow. Journal of Colloid and Interfacial Science, 16, 238-261.
- Schnabel, W. (1981). Polymer degradation: The principles and practical applications. New York: Hanser.
- Schoolenberg, G. E., During, F., and Ingenbleek, G. (1998). Coalescence and Interfacial tension measurements for polymer melts: Experiments on PS-PE model system. Polymer, 39, 765-772.
- Scott, C. E., and Macosko, C. W. (1995). Morphology development during the initial stages of polymer-polymer blending. Polymer, 36, 461-470.
- Sigillo, I., De Santo, L., Guido, S., and Grizuti, N. (1997). Comparative measurements of interfacial tension in a model polymer blend. Polymer Engineering and Science, 37, 1540-1549.
- Sundararaj, U., Macosko, C. W. (1995). Drop breakup and coalescence in polymer blends: The effects of concentration and compatibilization. Macromolecules, 28, 2647-2657.
- Sundararaj, U., Macosko, C. W., Rolando, R. J., and Chan, H. T. (1992). Morphology development in polymer blends. Polymer Engineering and Science, 32, 1814-1823.
- Tavgac T. (1972). Ph.D. Thesis, Faculty of Chemical Engineering, University of Houston, Houston, Texas.

- Taylor, G. I. (1934). The formation of emulsions in definable fields of flow. Proceedings of the Royal Society of London, A146, 501-523.
- Thomas, S., and Prud'homme, R. E. (1992). Polymer, 33, 4260.
- Tomokita, S. (1935). On the instability of a cylindrical thread of a viscous liquid surrounded by another viscous fluid. Proceedings of the Royal Society of London, A150, 322.
- Utracki, L. A. (1989). Polymer alloys and blends: Thermodynamics and rheology. New York: Hanser.
- Van Gisbergen, J. (1991). Ph.D. Thesis, Eindhoven University of Technology, Eindhoven, The Netherlands.
- Varanasi, P. P., Ryan, M. E., and Stroeve, P. (1994). Experimental study on the breakup of model viscoelastic drops in uniform shear flow. Ind. Eng. Chem. Res. 33, 1858-1866.
- Yang, K., and Han, C. D. (1996). Effects of shear flow and annealing on the morphology of rapidly precipitated immiscible blends of polystyrene and isoprene. Polymer, 37, 5795-5805.
- Wu, S. (1987). Formation of dispersed phase in incompatible polymer blends: Interfacial and rheological effect. Polymer Engineering and Science, 27(5), 335-343.

## APPENDIX A

### THE RHEOLOGY CHARACTERIZATIONS

**Table A1** The molecular weight characterization data by the rheological method

Material Type	PS	PP
Test Temperature (°C)	160	190
Relaxation Time Exponent	3.4	3.6
Plateau Modulus (dyn/cmsq)	1.7E+06	4.5E+06
Activation Energy (kJ/mol K)	57	42
Front Factor	7.9E-08	2.01E-22
Entanglement $M_w$ (g/mol)	17400	6520
Reptation $M_w$ (g/mol)	35000	13040

Mixing Rule

Double Reptation

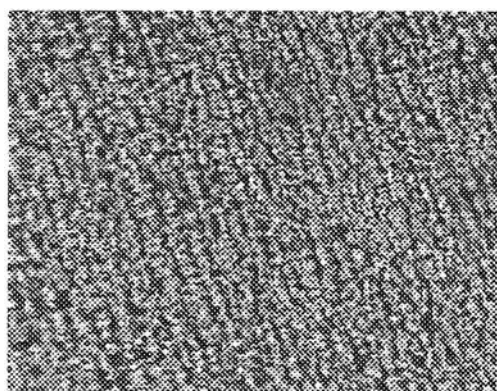
Polymer	T (°C)	Molecular weight (g/mole)						Polydispersity		
		$M_w$			$M_n$			1	2	AVG.
		1	2	AVG.	1	2	AVG.			
PP(1)	190	7.16E+06	8.79E+06	7.98E+06	3.41E+05	3.40E+05	3.41E+05	21.0	25.9	23.4
Company		8.53E+06			4.40E+05			19.4		
PP(2)	190	6.67E+06	7.50E+06	7.09E+06	3.50E+05	3.14E+05	3.32E+05	19.1	23.9	21.5
Company		7.35E+06			3.60E+05			20.4		
PP(3)	190	6.29E+06	6.10E+06	6.20E+06	3.08E+05	2.15E+05	2.62E+05	20.4	28.4	24.4
Company		6.78E+06			5.43E+05			12.5		
PP(4)	190	4.59E+06	4.32E+06	4.46E+06	2.21E+05	2.08E+05	2.15E+05	20.8	20.8	20.8
Company		5.10E+06			3.31E+05			15.4		
PS(1)	160	2.34E+05	2.89E+05	2.62E+05	9.59E+04	1.49E+05	1.22E+05	2.4	1.9	2.2
Company		-			-			-		
PS(2)	160	1.84E+05	1.54E+05	1.69E+05	5.58E+04	2.95E+04	4.27E+04	3.3	5.2	4.3
Company		-			-			-		
PS(3)	160	8.40E+04	7.69E+04	8.05E+04	2.73E+03	2.71E+03	2.72E+03	30.8	28.4	29.6
Company		-			-			-		

**Table A2** The zero shear viscosity of the homopolymer at 220 °C

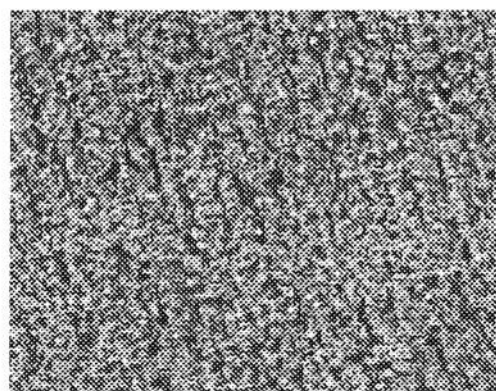
Polymers	Zero shear viscosity (Poise)					AVG. (Poise)
	1	2	3	4	5	
PP(1)	1.04E+05	9.83E+04	9.54E+04	8.12E+04	8.93E+04	9.36±0.87 (x 10 <sup>4</sup> )
PP(2)	5.98E+04	6.66E+04	6.18E+04	6.76E+04	6.03E+04	6.32±0.36 (x 10 <sup>4</sup> )
PP(3)	4.45E+04	4.42E+04	4.46E+04	4.43E+04	4.42E+04	4.44±0.02 (x 10 <sup>4</sup> )
PP(4)	1.85E+04	1.65E+04	1.90E+04	1.61E+04	1.80E+04	1.76±0.13 (x 10 <sup>4</sup> )
PS(1)	1.27E+05	1.27E+05	1.27E+05	1.26E+05	1.27E+05	1.27±0.04 (x 10 <sup>5</sup> )
PS(2)	1.51E+04	1.76E+04	1.36E+04	1.36E+04	1.49E+04	1.50±0.16 (x 10 <sup>4</sup> )
PS(3)	9.07E+03	8.42E+03	9.73E+03	9.34E+03	9.12E+03	9.14±0.47 (x 10 <sup>3</sup> )

**APPENDIX B**  
**MICROGRAPHS OF THE BLENDS**

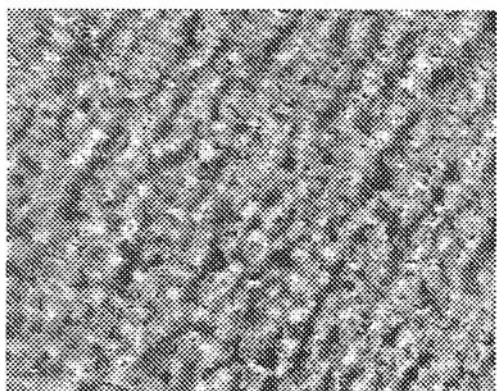
**Figure B1** Micrographs of the PS/PP blends of various thicknesses at the shear strain rate of  $10\text{ s}^{-1}$ ,  $220\text{ }^{\circ}\text{C}$ , magnification: 500 times.



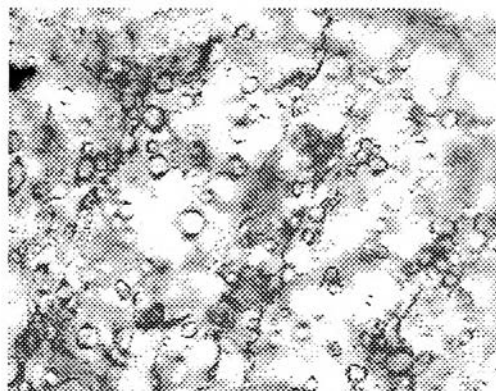
Thickness = 10  $\mu\text{m}$



Thickness = 12  $\mu\text{m}$

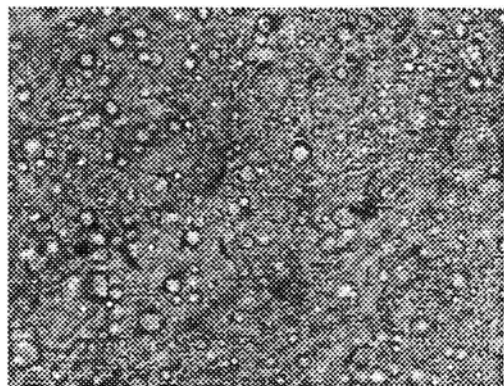


Thickness = 14  $\mu\text{m}$

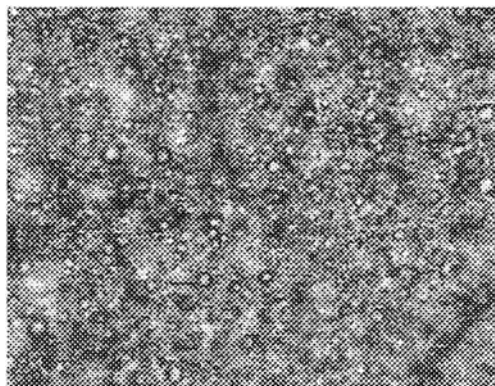


Thickness = 16  $\mu\text{m}$

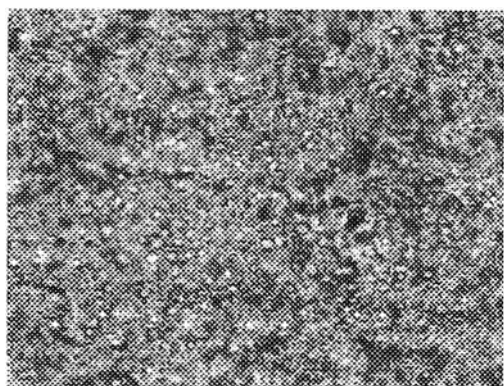
**Figure B2** Micrographs of PS(2)/PP(3) blends at various shearing times at the shear strain rate of  $10 \text{ s}^{-1}$ , and at  $220 \text{ }^{\circ}\text{C}$ , magnification: 500 times. (Figure 4.5)



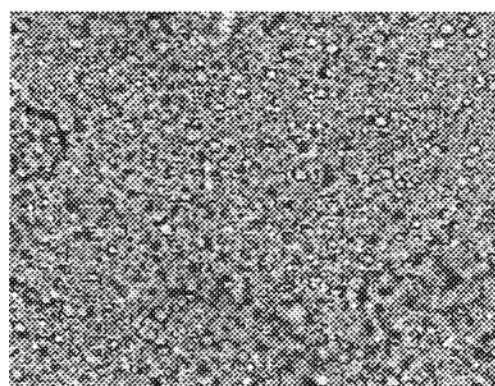
Shearing time = 300 s



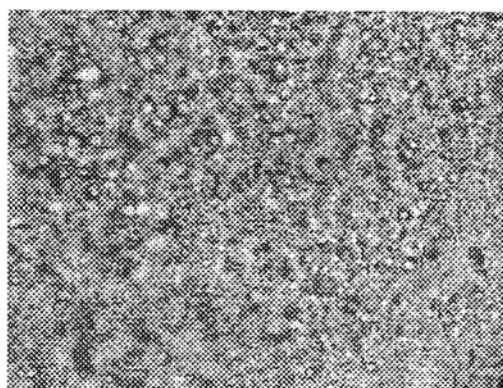
Shearing time = 500 s



Shearing time = 1000 s



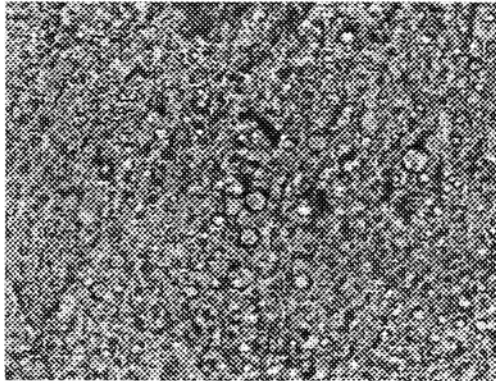
Shearing time = 1500 s



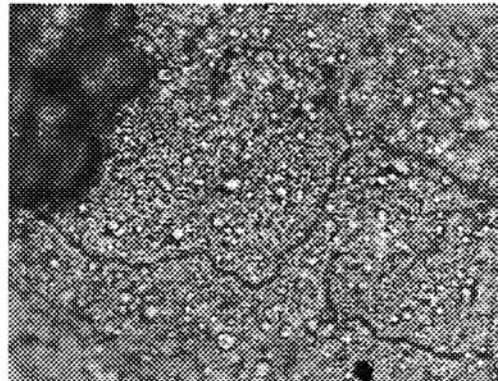
Shearing time = 2000 s



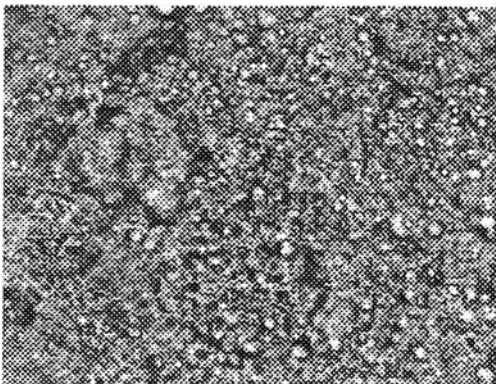
**Figure B3** Micrographs of PS(2)/PP(3) blends at various shearing times at the shear strain rate  $100\text{ s}^{-1}$ , and at  $220\text{ }^{\circ}\text{C}$ , magnification: 500 times. (Figure 4.5)



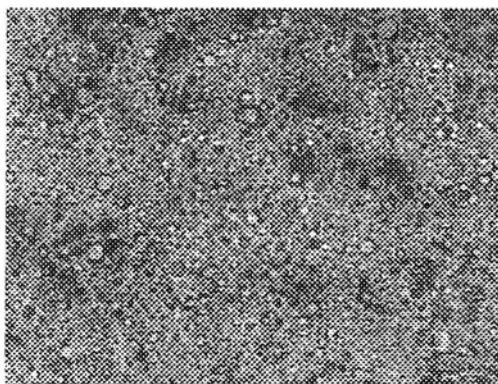
Shearing time = 30 s



Shearing time = 50 s



Shearing time = 100 s

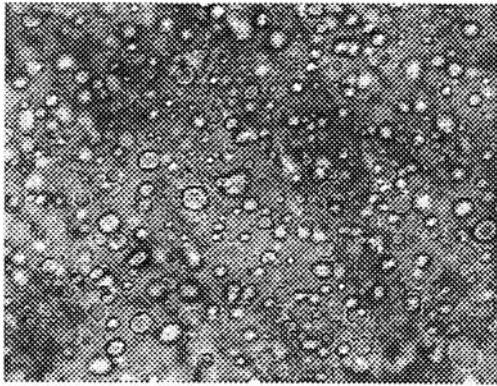


Shearing time = 150 s

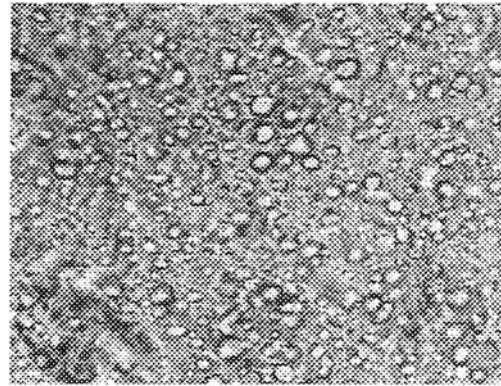


Shearing time = 200 s

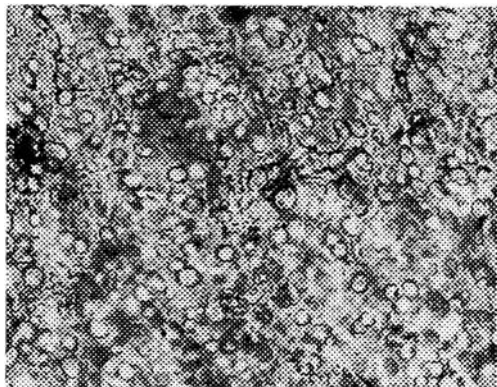
**Figure B4** Micrographs of PS(1)/PP(4) blends at various shearing times at the shear strain rate  $10\text{ s}^{-1}$ , and at  $220\text{ }^{\circ}\text{C}$ , magnification: 500 times. (Figure 4.5)



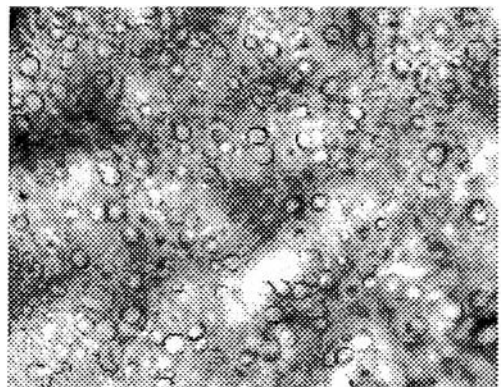
Shearing time = 300 s



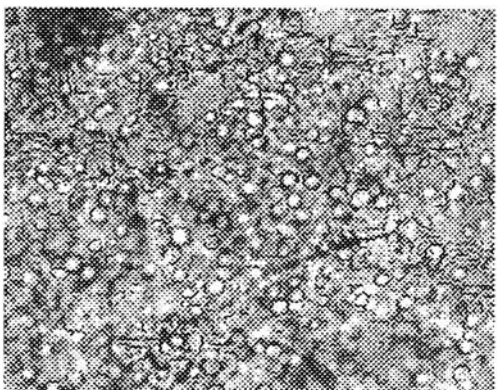
Shearing time = 500 s



Shearing time = 1000 s

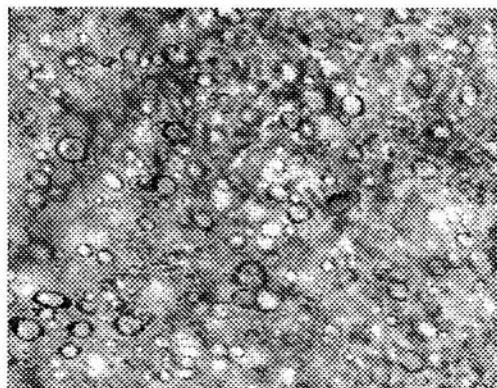


Shearing time = 1500 s

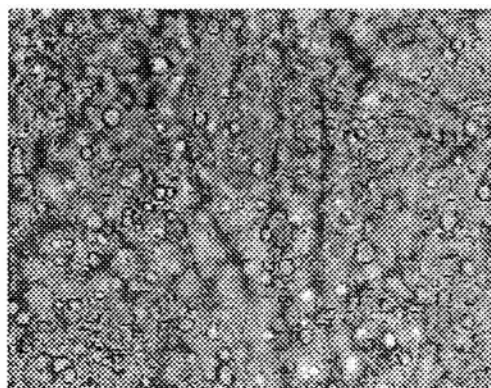


Shearing time = 2000 s

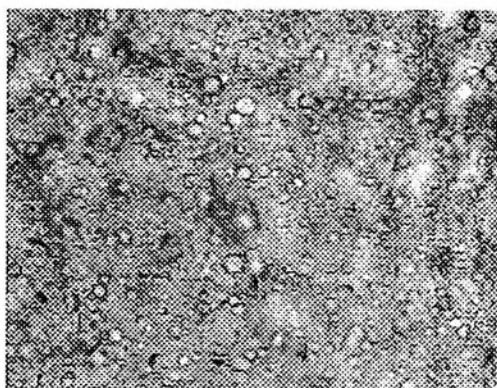
**Figure B5** Micrographs of PS(1)/PP(4) blends at various shearing times at the shear strain rate  $100\text{ s}^{-1}$ , and at  $220\text{ }^{\circ}\text{C}$ , magnification: 500 times. (Figure 4.5)



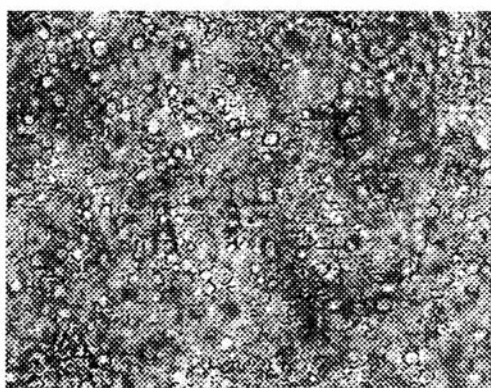
Shearing time = 30 s



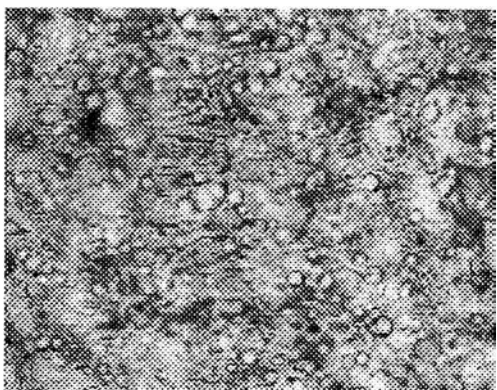
Shearing time = 50 s



Shearing time = 100 s

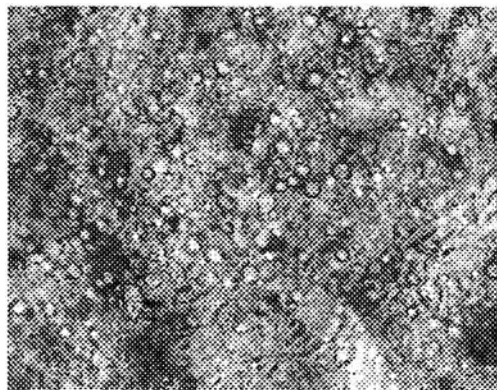


Shearing time = 150 s

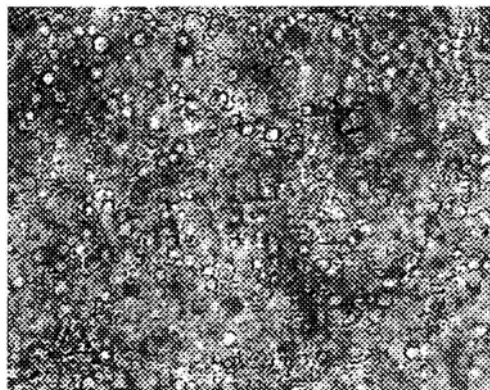


Shearing time = 200 s

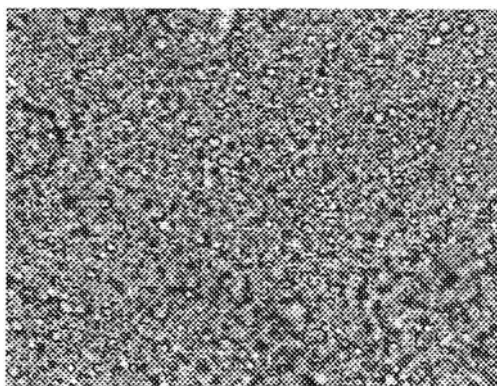
**Figure B6** Micrographs of PS(2)/PP(3) blends at various shear strain rates at 220 °C, magnification: 500 times. (Figure 4.11)



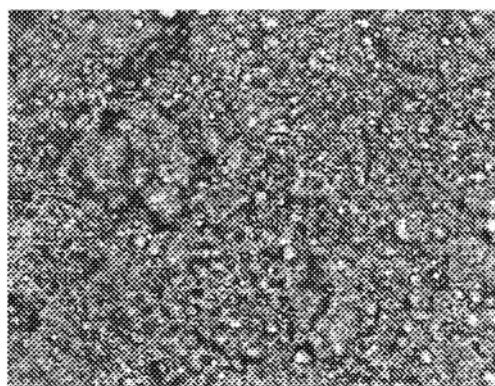
Shear strain rate = 10 s<sup>-1</sup>



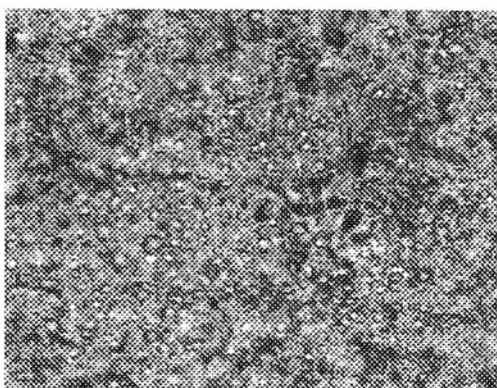
Shear strain rate = 30 s<sup>-1</sup>



Shear strain rate = 70 s<sup>-1</sup>

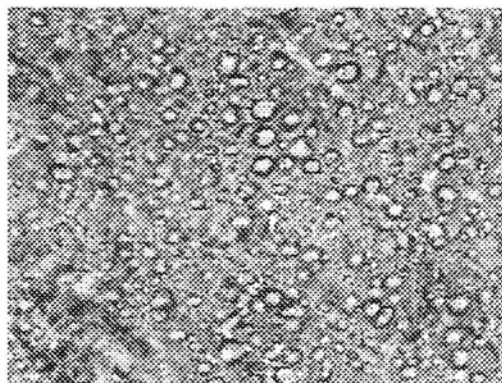


Shear strain rate = 100 s<sup>-1</sup>

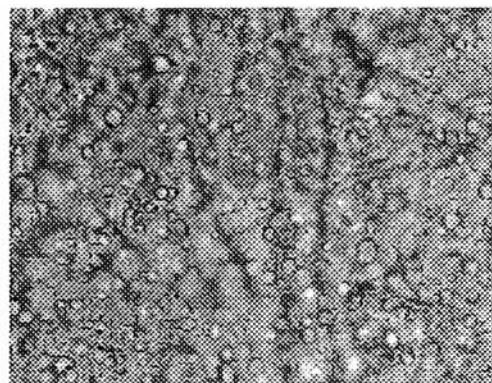


Shear strain rate = 200 s<sup>-1</sup>

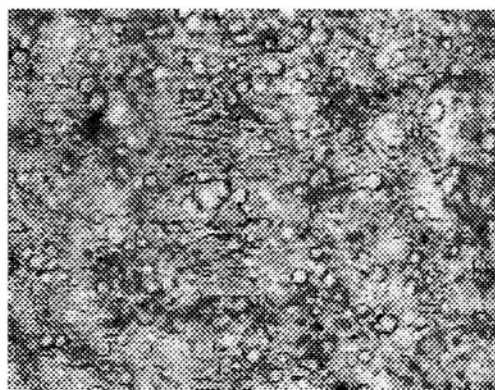
**Figure B7** Micrographs of PS(1)/PP(4) blends at various shear strain rates at 220 °C, magnification: 500 times. (Figure 4.11)



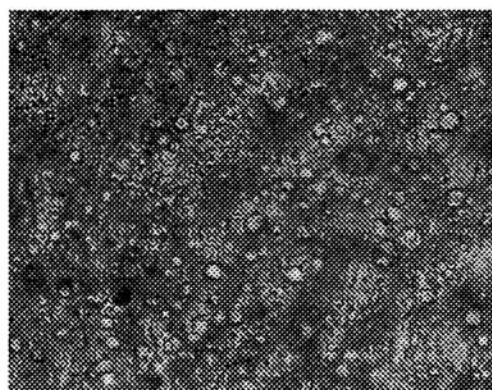
Shear strain rate = 10 s<sup>-1</sup>



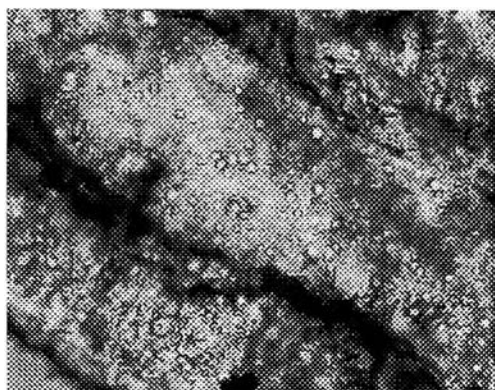
Shear strain rate = 30 s<sup>-1</sup>



Shear strain rate = 70 s<sup>-1</sup>



Shear strain rate = 100 s<sup>-1</sup>



Shear strain rate = 200 s<sup>-1</sup>

**APPENDIX C**  
**DROPLET SIZE DISTRIBUTION FUNCTIONS**

**Table C1** Droplet size distribution functions for PS(1)/PP(4) at the shear strain rate of  $10 \text{ s}^{-1}$ ,  $220 \text{ }^{\circ}\text{C}$  (Figure 4.7)

Shearing time									
300 s		500 s		1000 s		1500 s		2000 s	
d	f(d)	d	f(d)	d	f(d)	d	f(d)	d	f(d)
6.125	0.0000	4.875	0.0000	5.875	0.0000	5.625	0.0000	5.125	0.0000
6.375	0.0511	5.125	0.0073	6.375	0.0543	6.375	0.0730	6.375	0.0800
6.875	0.0876	6.375	0.0584	6.875	0.1783	6.875	0.1679	6.875	0.2320
7.625	0.1679	6.875	0.1168	7.625	0.5581	7.625	0.5255	7.625	0.4320
8.125	0.0876	7.625	0.2409	8.125	0.1628	8.125	0.1533	8.125	0.1680
8.375	0.0146	8.125	0.1241	8.875	0.0465	8.875	0.0803	8.875	0.0880
8.625	0.0511	8.625	0.0876	9.375	0.0000	9.625	0.0000	9.625	0.0000
8.875	0.0876	8.875	0.1387						
9.125	0.3796	9.125	0.1168						
9.375	0.0365	9.375	0.0219						
9.875	0.0073	9.875	0.0073						
10.125	0.0000	10.125	0.0000						









**Table C5** Droplet size distribution functions for PS(1)/PP(4) as a function of shear strain rate at 220 °C (Figure 4.12)

Shear strain rate (s <sup>-1</sup> )									
10		30		70		100		200	
d	f(d)	d	f(d)	d	f(d)	d	f(d)	d	f(d)
5.625	0.0000	4.125	0.0000	2.875	0.0000	2.125	0.0000	1.875	0.0000
6.375	0.0730	4.625	0.0584	3.125	0.0185	3.125	0.0243	2.375	0.2063
6.875	0.1679	5.375	0.2409	3.625	0.0148	3.375	0.1505	3.125	0.4260
7.625	0.5255	5.875	0.1898	4.375	0.1519	3.875	0.2039	3.875	0.1794
8.125	0.1533	6.875	0.0730	4.875	0.2593	4.375	0.2524	4.375	0.0852
8.875	0.0803	7.625	0.0219	5.125	0.1148	4.875	0.1117	5.125	0.0045
9.625	0.0000	8.125	0.0000	5.625	0.0148	5.125	0.0146	5.625	0.0045
				5.875	0.0000	5.625	0.0049	5.875	0.0000
						5.875	0.0000		

**Table C6** Droplet size distribution functions for PS(2)/PP(3) as a function of shear strain rate at 220 °C (Figure 4.13)

Shear strain rate ( $s^{-1}$ )									
10		30		70		100		200	
d	f(d)	d	f(d)	d	f(d)	d	f(d)	d	f(d)
1.875	0.0000	1.625	0.0000	1.375	0.0000	0.875	0.0000	0.625	0.0000
2.375	0.0918	2.125	0.0635	1.625	0.0561	1.125	0.0368	0.875	0.0285
3.125	0.5102	2.375	0.1637	1.875	0.1429	1.375	0.0784	1.125	0.3264
3.875	0.3469	2.625	0.4133	2.125	0.6837	1.625	0.1618	1.625	0.2383
4.375	0.0459	3.125	0.5102	2.375	0.1173	2.125	0.2868	1.875	0.1425
4.625	0.0051	3.375	0.2635	2.625	0.0000	2.375	0.1127	2.125	0.0907
5.125	0.0000	3.625	0.0876			2.875	0.0319	2.375	0.0751
		3.875	0.0000			3.125	0.0123	2.625	0.0000
						3.375	0.0024		
						3.625	0.0000		

**Table C7** The ensemble averages of droplet size of PS/PP blends at 220 °C (Figure 4.5)

Polymer pairs	shear strain rate (s <sup>-1</sup> )	Droplet size	Shear strain unit				
			3000	5000	10000	15000	20000
PS(1)/PP(4)	10	AVG. (μm)	8.36	8.01	7.57	7.57	7.53
		STD.	0.91	0.9	0.57	0.63	0.67
		Max. (μm)	9.86	9.86	8.86	8.86	8.86
		Min. (μm)	6.26	5.10	6.26	6.26	6.26
	100	AVG. (μm)	4.87	4.01	3.36	3.42	3.40
		STD.	1.01	0.82	0.34	0.32	0.30
		Max. (μm)	6.79	5.7	4.43	4.43	4.43
		Min. (μm)	3.05	2.49	2.04	2.49	2.49
PS(2)/PP(3)	10	AVG. (μm)	4.62	3.7	3.33	3.39	3.36
		STD.	0.92	0.85	0.50	0.62	0.58
		Max. (μm)	6.39	5.83	4.55	4.55	4.55
		Min. (μm)	3.05	2.49	2.49	2.49	2.49
	100	AVG. (μm)	2.45	2.14	1.98	1.97	2.02
		STD.	0.76	0.52	0.41	0.41	0.50
		Max. (μm)	4.42	3.47	3.32	3.2	3.47
		Min. (μm)	1.01	1.01	1.01	1.01	0.87

**Table C8** The ensemble averages droplet size of PS/PP blends as a function of shear strain rate at 220 °C (Figure 4.11)

Polymer pairs	Statistical equilibrium	Shear strain rate (s <sup>-1</sup> )				
		10	30	70	100	200
PS(1)/PP(4)	AVG (μm)	7.58	5.68	4.48	3.9	3.24
	STD.	0.62	0.61	0.53	0.78	0.6
	Max (μm)	8.86	7.6	5.71	5.71	5.71
	Min (μm)	6.27	4.57	3.05	2.49	2.49
PS(2)/PP(3)	AVG (μm)	3.33	2.73	2.14	1.99	1.55
	STD.	0.5	0.35	0.21	0.41	0.41
	Max (μm)	4.55	3.05	2.49	3.31	2.44
	Min (μm)	2.49	2.26	1.61	1.01	0.82

**Figure C1** Distribution function of droplet size of PS(1)/PP(4) at shear strain rate of  $10 \text{ s}^{-1}$ ,  $220 \text{ }^\circ\text{C}$  (Figure 4.7).

Compression conditions:

Heating temperature :  $175 \text{ }^\circ\text{C}$   
 Preheating time : 5 min  
 Load : 10 tons  
 Compression time under load: 3 min  
 Cooling temperature :  $40 \text{ }^\circ\text{C}$

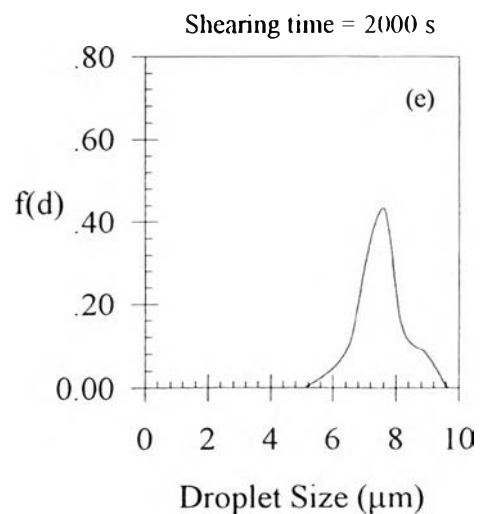
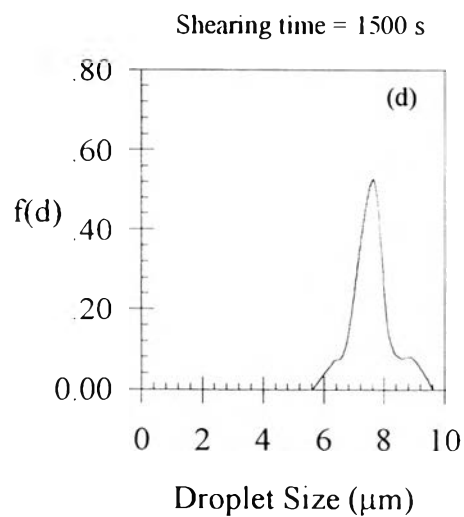
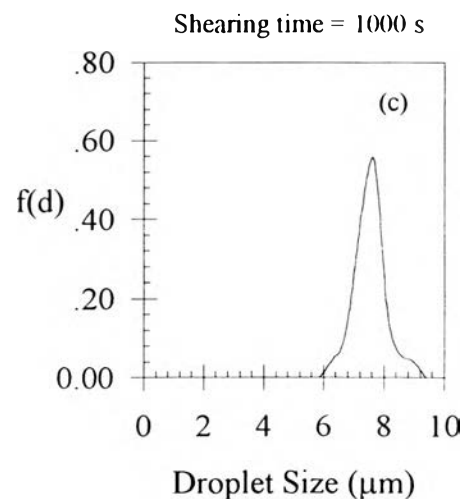
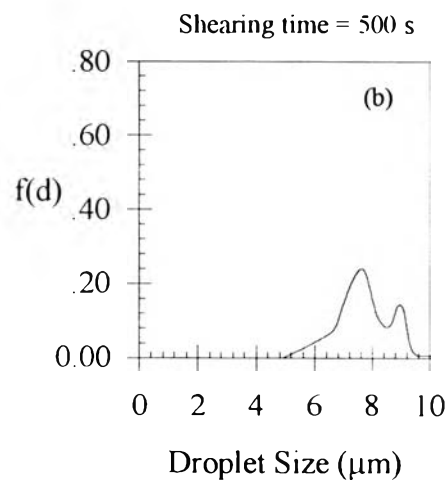
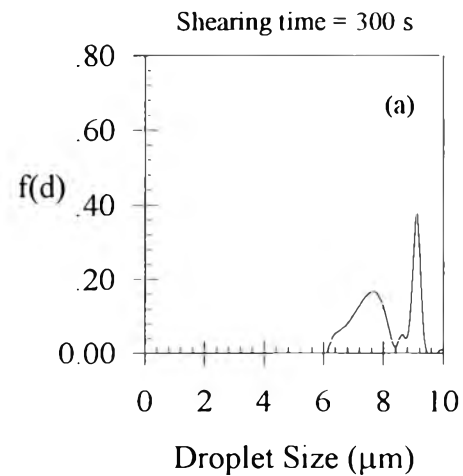


**Figure C2** Distribution function of droplet size of PS(1)/PP(4) at the shear strain rate of  $100 \text{ s}^{-1}$ ,  $220^\circ\text{C}$  (Figure 4.8).

Compression conditions:

Heating temperature :  $175^\circ\text{C}$   
 Preheating time : 5 min  
 Load : 10 tons  
 Compression time under load: 3 min  
 Cooling temperature :  $40^\circ\text{C}$

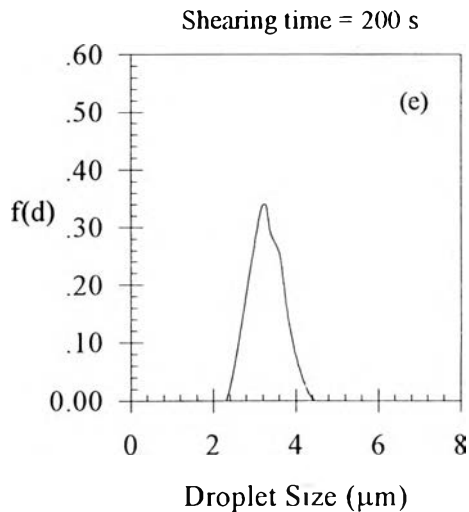
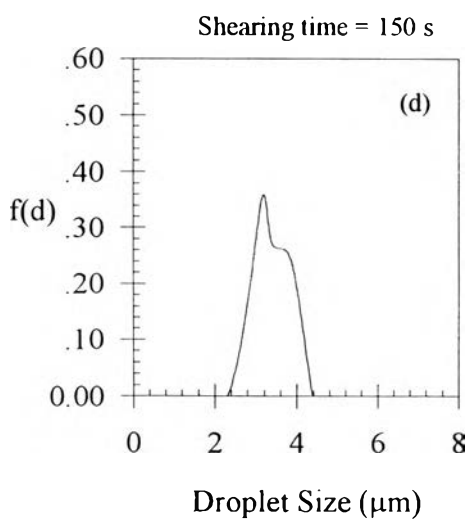
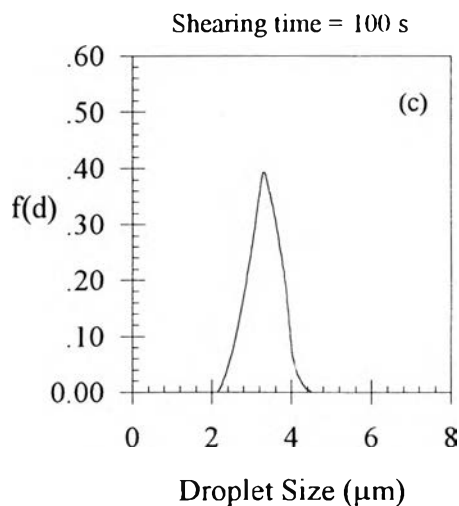
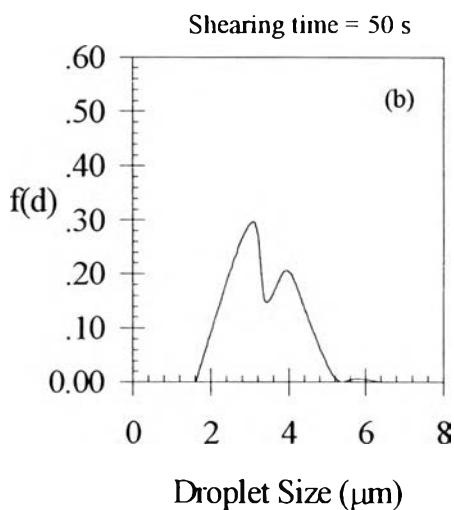
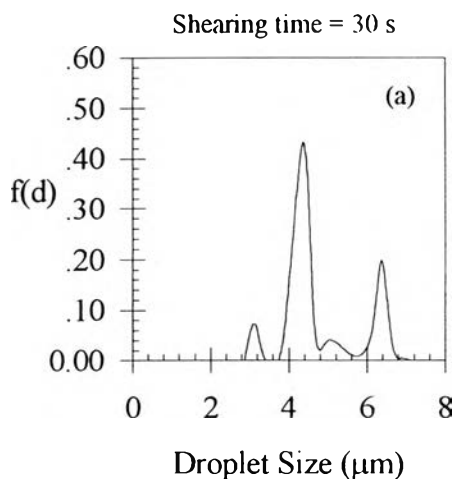


**Figure C3** Distribution function of droplet size of PS(2)/PP(3) at the shear strain rate of  $10 \text{ s}^{-1}$ ,  $220 \text{ }^{\circ}\text{C}$  (Figure 4.9).

Compression conditions:

Heating temperature :  $175 \text{ }^{\circ}\text{C}$   
 Preheating time : 5 min  
 Load : 10 tons  
 Compression time under load: 3 min  
 Cooling temperature :  $40 \text{ }^{\circ}\text{C}$

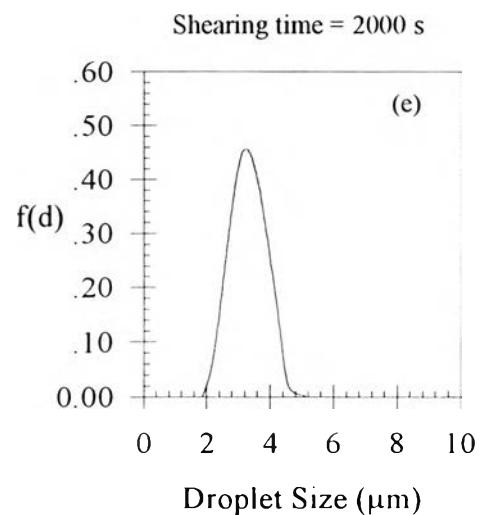
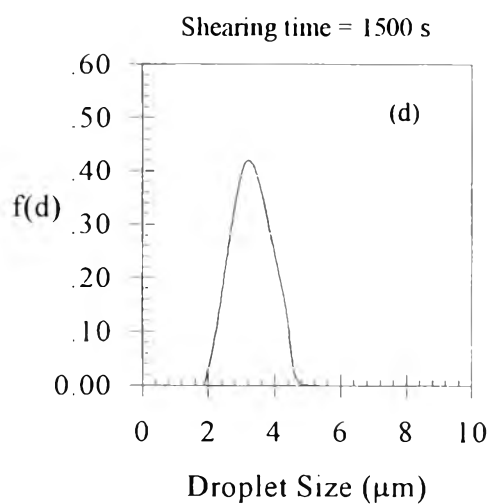
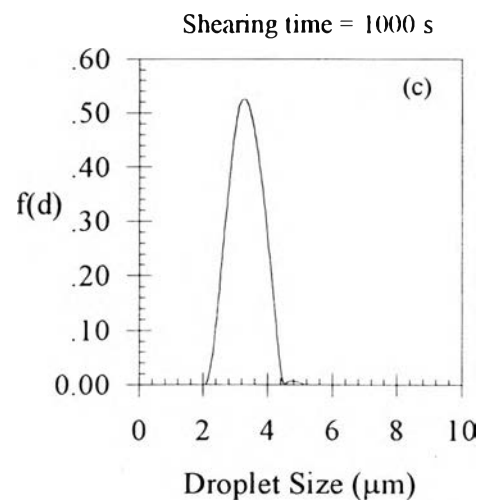
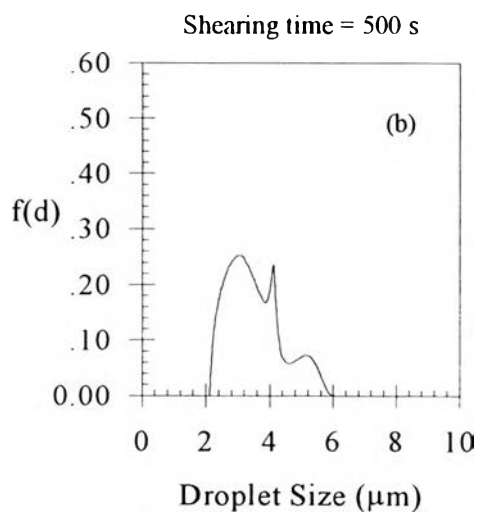
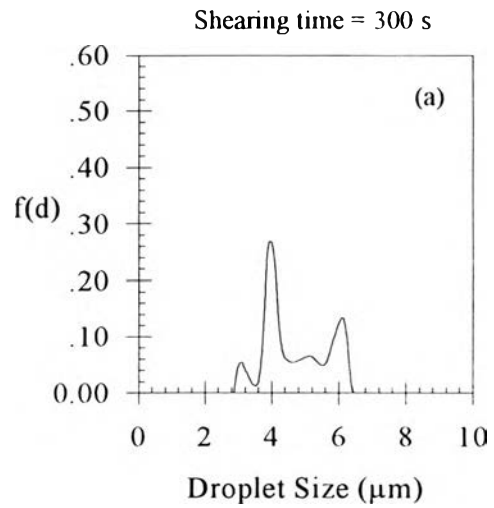


**Figure C4** Distribution function of droplet size of PS(2)/PP(3) at the shear strain rate of  $100 \text{ s}^{-1}$ ,  $220^\circ\text{C}$  (Figure 4.10).

Compression conditions:

Heating temperature :  $175^\circ\text{C}$   
 Preheating time : 5 min  
 Load : 10 tons  
 Compression time under load: 3 min  
 Cooling temperature :  $40^\circ\text{C}$

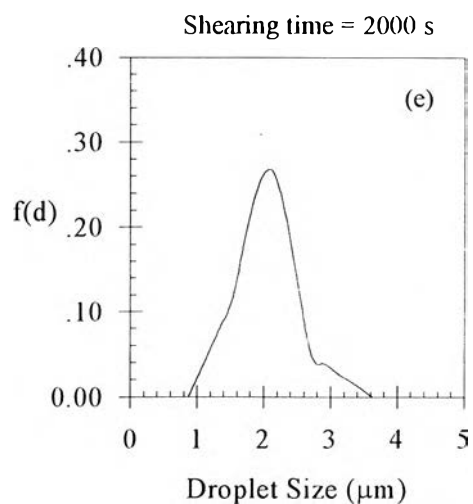
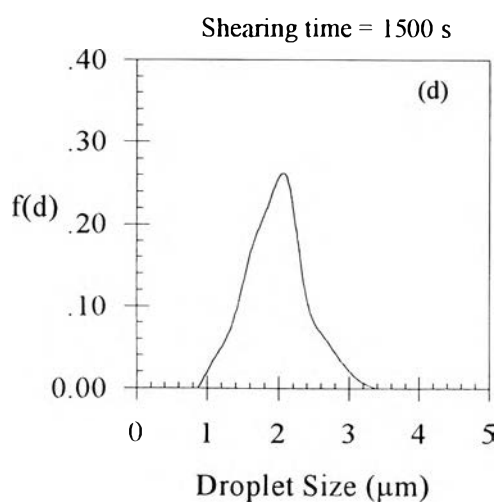
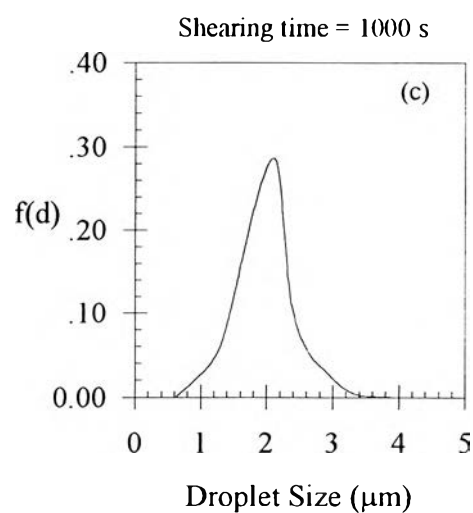
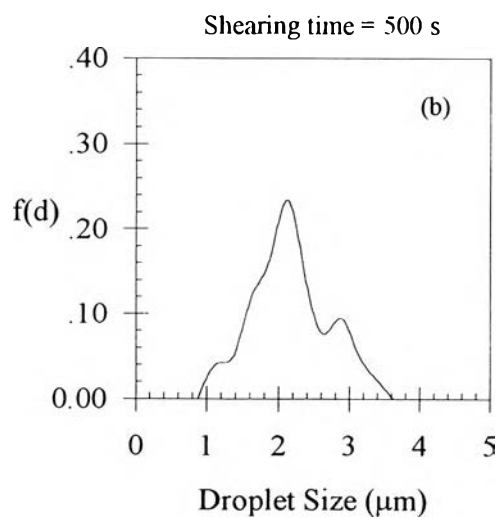
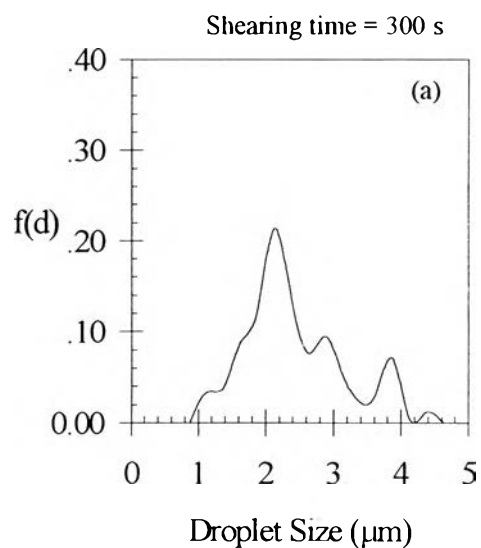




**Figure C5** Distribution function of droplet size of PS(1)/PP(4) as a function of shear strain rate at 220 °C (Figure 4.12).

Compression conditions:

Heating temperature : 175 °C  
 Preheating time : 5 min  
 Load : 10 tons  
 Compression time under load: 3 min  
 Cooling temperature : 40 °C

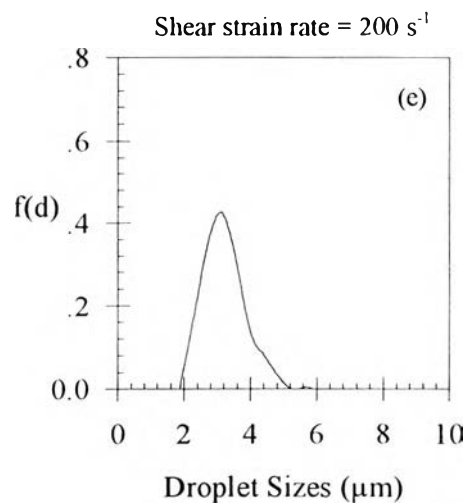
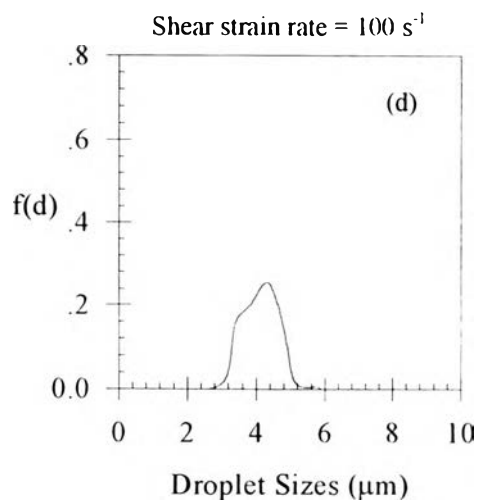
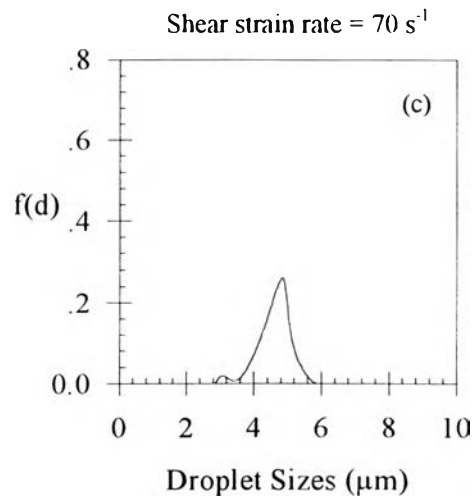
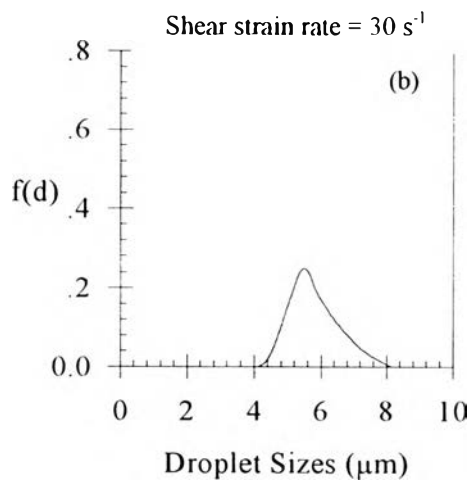
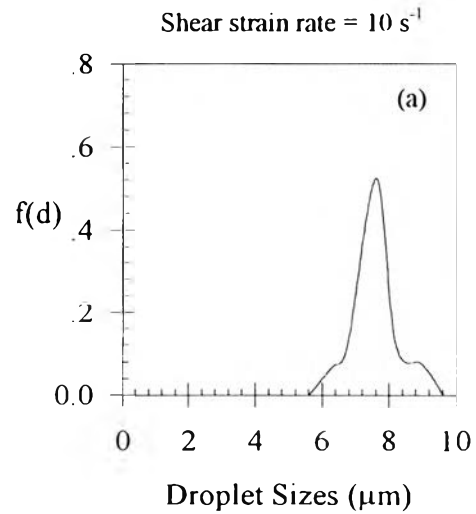
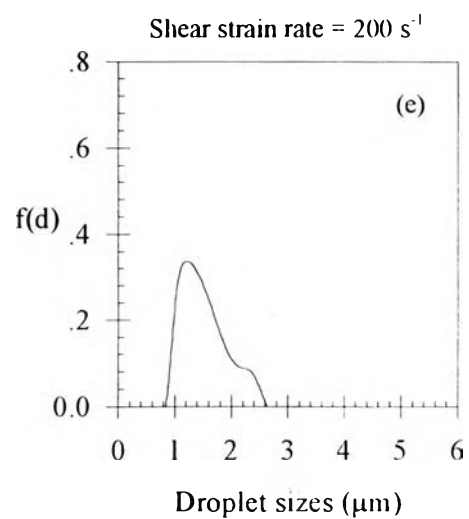
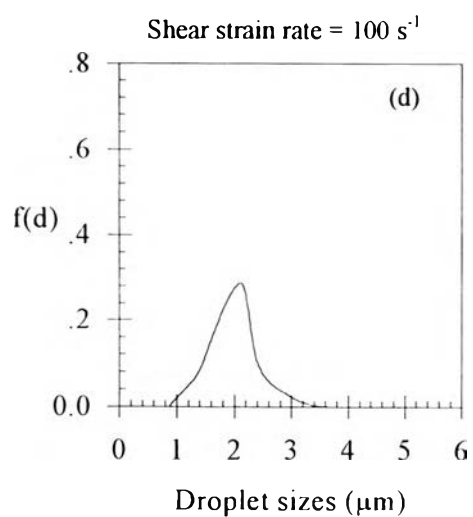
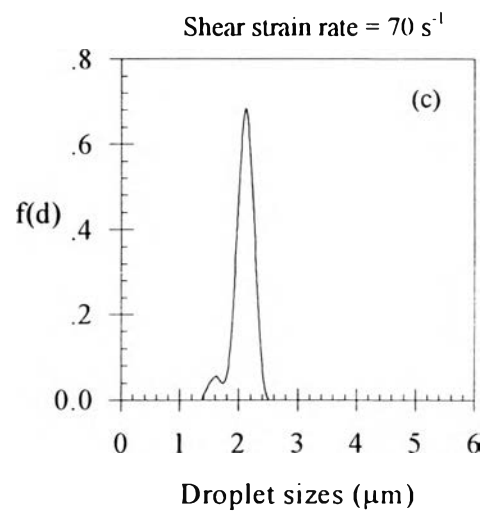
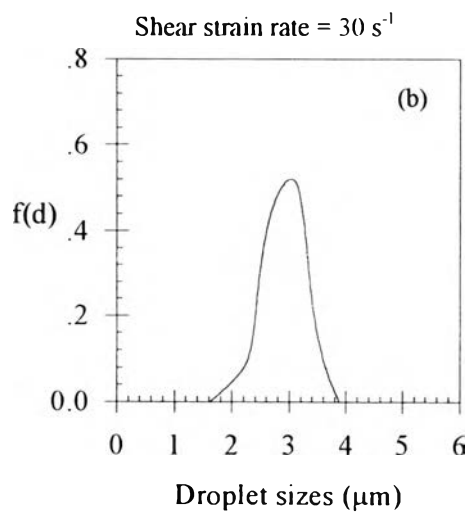
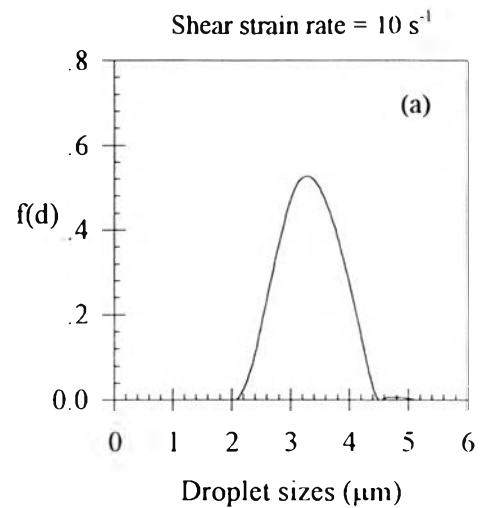


**Figure C6** Distribution function of droplet size of PS(2)/PP(3) as a function of shear strain rate at 220 °C (Figure 4.13).

Compression conditions:

Heating temperature : 175 °C  
 Preheating time : 5 min  
 Load : 10 tons  
 Compression time under load: 3 min  
 Cooling temperature : 40 °C



## APPENDIX D

### INTERFACIAL TENSION OF PS/PP BLENDS

The interfacial tension,  $\Gamma_{12}$ , between 2 homopolymers making up an immiscible blend was calculated from the surface tension of each component, assuming that no chemical reaction took place. Both surface and interfacial tension decrease with increasing temperature. The values of surface tension for the homopolymers have been published (Brandrup, 1989). The surface tension of a polymer at any temperature can be calculated from the temperature coefficient of surface tension and surface tension at a reference temperature as

$$\gamma_T = \gamma_r - \frac{d\gamma}{dT}(T - 20) \quad (D-1)$$

where  $\gamma_T$  is the surface tension at a required temperature,  $\gamma_r$  is the surface tension at a reference temperature,  $(d\gamma/dT)$  is a temperature coefficient, and  $T$  is the temperature ( $^{\circ}\text{C}$ ). The surface tension consists of disperse-contribution and polar-contribution

$$\gamma = \gamma^d + \gamma^p \quad (D-2)$$

$$\chi^p = \frac{\gamma^p}{\gamma} \quad (D-3)$$

$$\chi^d = \frac{\gamma^d}{\gamma} \quad (D-4)$$

$$\chi^p + \chi^d = 1 \quad (D-5)$$

where  $\gamma^d$  is dispersion component (arising from dispersion force interactions),  $\gamma^p$  is polar component (arising from various dipolar and specific interactions),  $\chi^p$  is the polarity of polymers (depending on chemical structure of polymer), and  $\chi^d$  is the dispersion value of polymers. The interfacial tension is related to

the surface tension and the polarity of two contiguous phase by the harmonic-mean equation.

$$\Gamma_{12} = \gamma_1 + \gamma_2 - \frac{4\gamma_1^d \gamma_2^d}{\gamma_1^d + \gamma_2^d} - \frac{4\gamma_1^p \gamma_2^p}{\gamma_1^p + \gamma_2^p} \quad (\text{D-6})$$

where  $\Gamma_{12}$  is an interfacial tension between polymer pair, the subscripts 1 and 2 refer to the two individual phases. The harmonic-mean equation has been shown to predict the interfacial tension between polymers satisfactorily.

The surface tension and interfacial tension at temperature 220 °C are shown in Table D1 and D2, respectively.

**Table D1** Surface tension of homopolymer at 20, 150 and 200°C

Polymers	$\gamma$ (dyn/cm)			$\chi^p$	$\chi^d$	$\gamma^d$			$\gamma^p$		
	20°C	150°C	200°C			20°C	150°C	200°C	20°C	150°C	200°C
PP	29.4	22.1	19.3	0	1	0	0	0	29.4	22.1	19.3
PS	40.7	31.4	27.8	0.17	0.83	6.8	5.2	4.6	33.8	26.1	23.1

**Table D2** The interfacial tension of PS/PP blends at 20, 150 and 200°C

Polymer blend system	$\Gamma_{12}$ of PS/PP (dyn/cm)				$\Gamma_{12}$ from references <sup>@</sup> at 220 °C (dyn/cm)
	20°C *	150°C *	200°C *	220°C +	
PS/PP	7.15	5.61	5.02	4.78	5.00

\* from calculation

+ from Figure D1

@ Levitt *et al.*, 1996

The surface tension of polymer is usually a linear function of temperature. The interfacial tension is found to decrease linearly with temperature. So the interfacial tension of PS/PP blends at 220°C are also obtained from the relation of interfacial tension and temperature as shown in Figure D1. From the linear regression, the interfacial tension of PS/PP blends at 220 °C is 4.78 dyn/cm.

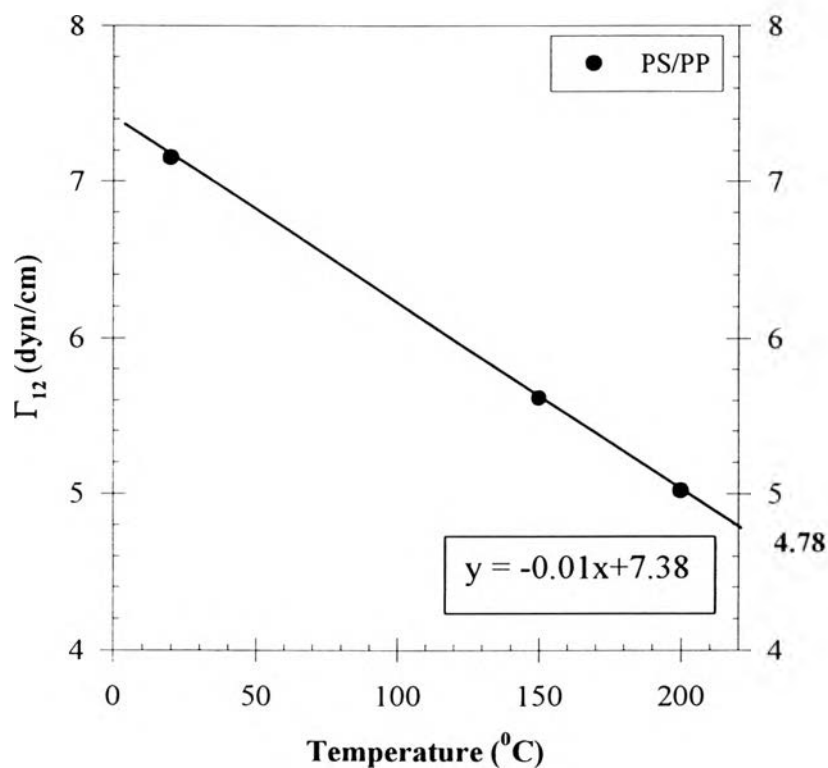


**Figure D1** The interfacial tension of PS/PP blends as a function of temperature.

**Table E1** The dimensionless parameters for PS/PP blends of pre-shearing at the viscosity ratio of 0.5, 220 °C (Figure 4.14)

Polymer pairs	$\Gamma^*$ (dyn/cm)	$\gamma$ (s <sup>-1</sup> )	D ( $\mu$ m)	$\eta_d$ (Poise)	$\eta_m$ (Poise)	$\eta_r$	$N_{1,d}$ (dyn/cm <sup>2</sup> )	$N_{1,m}$ (dyn/cm <sup>2</sup> )	$N_{1,r}$	Ca
PS(3)/PP(3)	4.78	30	3.21 $\pm$ 0.65	3.78E+04	7.13E+04	0.53	1.90E+05	5.57E+05	0.34	14.36 $\pm$ 2.91
PS(2)/PP(3)	4.78	10	5.16 $\pm$ 1.44	6.82E+04	1.42E+05	0.48	9.23E+04	2.50E+05	0.37	15.34 $\pm$ 4.27
PS(2)/PP(3)	4.78	20	3.97 $\pm$ 1.72	5.17E+04	1.09E+05	0.47	1.75E+05	4.33E+05	0.40	18.12 $\pm$ 7.84
PS(3)/PP(3)	4.78	50	3.48 $\pm$ 0.88	2.89E+04	5.44E+04	0.53	3.02E+05	6.16E+05	0.49	19.82 $\pm$ 5.02
PS(2)/PP(1)	4.78	50	4.07 $\pm$ 1.11	3.25E+04	6.09E+04	0.53	3.94E+05	7.16E+05	0.55	25.92 $\pm$ 7.08

\* calculated from Harmonic equation (Appendix D)

**Table E2** The dimensionless parameters for PS/PP blends of pre-shearing at the viscosity ratio of 1, 220 °C (Figure 4.14)

Polymer pairs	$\Gamma^*$ (dyn/cm)	$\gamma$ (s <sup>-1</sup> )	D ( $\mu$ m)	$\eta_d$ (Poise)	$\eta_m$ (Poise)	$\eta_r$	$N_{1,d}$ (dyn/cm <sup>2</sup> )	$N_{1,m}$ (dyn/cm <sup>2</sup> )	$N_{1,r}$	Ca
PS(3)/PP(2)	4.78	30	1.43 $\pm$ 0.30	3.22E+04	4.08E+04	0.79	1.40E+05	4.01E+05	0.35	3.66 $\pm$ 0.76
PS(2)/PP(2)	4.78	20	1.60 $\pm$ 0.48	4.86E+04	5.92E+04	0.82	1.57E+05	3.82E+05	0.41	3.96 $\pm$ 1.20
PS(2)/PP(2)	4.78	30	1.70 $\pm$ 0.41	4.25E+04	4.08E+04	1.04	2.13E+05	4.01E+05	0.53	4.35 $\pm$ 1.04
PS(3)/PP(3)	4.78	100	1.11 $\pm$ 0.36	2.13E+04	1.86E+04	1.14	4.64E+05	6.72E+05	0.69	4.32 $\pm$ 1.43
PS(3)/PP(4)	4.78	50	1.37 $\pm$ 0.38	3.45E+04	3.29E+04	1.05	3.33E+05	3.62E+05	0.92	4.71 $\pm$ 0.98
PS(2)/PP(4)	4.78	50	1.66 $\pm$ 0.42	2.77E+04	2.83E+04	0.98	4.05E+05	3.62E+05	1.12	4.91 $\pm$ 1.20

**Table E3** The dimensionless parameters for PS/PP blends of pre-shearing at the viscosity ratio of 2, 220 °C (Figure 4.14)

Polymer pairs	$\Gamma^*$ (dyn/cm)	$\gamma$ (s <sup>-1</sup> )	D ( $\mu\text{m}$ )	$\eta_d$ (Poise)	$\eta_m$ (Poise)	$\eta_r$	$N_{1,d}$ (dyn/cm <sup>2</sup> )	$N_{1,m}$ (dyn/cm <sup>2</sup> )	$N_{1,r}$	Ca
PS(2)/PP(2)	4.78	50	3.89 ± 0.89	3.25E+04	1.94E+04	1.68	3.91E+05	4.16E+05	0.94	7.88 ± 1.81
PS(3)/PP(4)	4.78	100	3.87 ± 1.03	1.99E+04	1.02E+04	1.95	4.98E+05	4.30E+05	1.16	8.25 ± 2.20
PS(1)/PP(3)	4.78	30	3.60 ± 0.92	1.35E+05	7.13E+04	1.90	8.39E+05	5.57E+05	1.51	15.88 ± 4.14
PS(1)/PP(3)	4.78	70	3.56 ± 1.16	7.46E+04	3.09E+04	2.41	1.08E+06	6.38E+05	1.68	16.11 ± 5.18

**Table E4** The dimensionless parameters for PS/PP blends of pre-shearing at the viscosity ratio of 3, 220 °C (Figure 4.14)

Polymer pairs	$\Gamma^*$ (dyn/cm)	$\gamma$ (s <sup>-1</sup> )	D ( $\mu\text{m}$ )	$\eta_d$ (Poise)	$\eta_m$ (Poise)	$\eta_r$	$N_{1,d}$ (dyn/cm <sup>2</sup> )	$N_{1,m}$ (dyn/cm <sup>2</sup> )	$N_{1,r}$	Ca
PS(1)/PP(2)	4.78	10	3.40 ± 0.93	2.83E+05	1.12E+05	2.53	3.85E+05	2.76E+05	1.40	7.94 ± 2.17
PS(1)/PP(3)	4.78	100	3.10 ± 0.74	5.60E+04	1.86E+04	3.01	9.83E+05	6.72E+05	2.33	11.32 ± 2.69
PS(1)/PP(4)	4.78	30	4.53 ± 1.03	1.45E+05	4.55E+04	3.19	9.39E+05	2.77E+05	3.39	12.94 ± 2.95
PS(1)/PP(4)	4.78	20	5.24 ± 1.04	1.90E+05	6.08E+04	3.12	9.12E+05	2.11E+05	4.31	13.33 ± 2.66

**Table E5** The dimensionless parameters for PS/PP blends after shearing 5000 strain unit at the viscosity ratio of 0.5, 220 °C (Figure 4.15)

Polymer pairs	$\Gamma^*$ (dyn/cm)	$\gamma$ (s <sup>-1</sup> )	D ( $\mu$ m)	$\eta_d$ (Poise)	$\eta_m$ (Poise)	$\eta_r$	$N_{1,d}$ (dyn/cm <sup>2</sup> )	$N_{1,m}$ (dyn/cm <sup>2</sup> )	$N_{1,r}$	Ca
PS(3)/PP(3)	4.78	30	3.21 $\pm$ 0.65	3.51E+03	6.88E+03	0.51	6.30E+04	1.97E+05	0.32	13.26 $\pm$ 2.68
PS(2)/PP(3)	4.78	10	5.16 $\pm$ 1.44	6.81E+03	1.31E+04	0.52	5.24E+04	1.50E+05	0.35	13.52 $\pm$ 3.77
PS(2)/PP(3)	4.78	20	3.97 $\pm$ 1.72	5.22E+03	1.02E+04	0.51	6.72E+04	1.64E+05	0.41	16.28 $\pm$ 7.04
PS(3)/PP(3)	4.78	50	3.48 $\pm$ 0.88	2.88E+03	5.33E+03	0.54	1.21E+05	2.58E+05	0.47	18.57 $\pm$ 4.71
PS(2)/PP(1)	4.78	50	4.07 $\pm$ 1.11	3.28E+03	6.56E+03	0.50	2.19E+05	4.30E+05	0.51	26.75 $\pm$ 7.29

**Table E6** The dimensionless parameters for PS/PP blends after shearing 5000 strain unit at the viscosity ratio of 1, 220 °C (Figure 4.15)

Polymer pairs	$\Gamma^*$ (dyn/cm)	$\gamma$ (s <sup>-1</sup> )	D ( $\mu$ m)	$\eta_d$ (Poise)	$\eta_m$ (Poise)	$\eta_r$	$N_{1,d}$ (dyn/cm <sup>2</sup> )	$N_{1,m}$ (dyn/cm <sup>2</sup> )	$N_{1,r}$	Ca
PS(3)/PP(2)	4.78	30	1.43 $\pm$ 0.30	3.47E+03	3.66E+03	0.95	1.08E+05	2.41E+05	0.45	3.28 $\pm$ 0.68
PS(2)/PP(2)	4.78	20	1.60 $\pm$ 0.48	5.16E+03	5.11E+03	1.01	1.05E+05	2.29E+05	0.46	3.43 $\pm$ 1.04
PS(2)/PP(2)	4.78	30	1.70 $\pm$ 0.41	4.24E+03	3.66E+03	1.16	1.49E+05	2.41E+05	0.62	3.90 $\pm$ 0.94
PS(3)/PP(3)	4.78	100	1.11 $\pm$ 0.36	1.99E+03	1.71E+03	1.16	2.10E+05	2.83E+05	0.74	3.98 $\pm$ 1.32
PS(3)/PP(4)	4.78	50	1.37 $\pm$ 0.38	2.87E+03	2.79E+03	1.03	1.74E+05	2.17E+05	0.80	4.01 $\pm$ 0.84
PS(2)/PP(4)	4.78	50	1.66 $\pm$ 0.42	3.24E+03	2.79E+03	1.16	2.19E+05	2.17E+05	1.01	4.85 $\pm$ 1.22



**Table E7** The dimensionless parameters for PS/PP blends after shearing 5000 strain unit at the viscosity ratio of 2, 220 °C (Figure 4.15)

Polymer pairs	$\Gamma^*$ (dyn/cm)	$\gamma$ (s <sup>-1</sup> )	D ( $\mu$ m)	$\eta_d$ (Poise)	$\eta_m$ (Poise)	$\eta_r$	$N_{1,d}$ (dyn/cm <sup>2</sup> )	$N_{1,m}$ (dyn/cm <sup>2</sup> )	$N_{1,r}$	Ca
PS(2)/PP(2)	4.78	50	3.89 $\pm$ 0.89	3.24E+03	1.70E+03	1.91	2.20E+05	2.50E+05	0.88	6.60 $\pm$ 1.51
PS(3)/PP(4)	4.78	100	3.87 $\pm$ 1.03	1.99E+03	1.02E+03	1.95	2.99E+05	2.58E+05	1.16	7.89 $\pm$ 2.10
PS(1)/PP(3)	4.78	30	3.60 $\pm$ 0.92	1.35E+04	6.88E+03	1.97	4.89E+05	1.97E+05	2.48	14.87 $\pm$ 3.82
PS(1)/PP(3)	4.78	70	3.56 $\pm$ 1.16	7.37E+03	3.76E+03	1.96	9.31E+05	2.73E+05	3.41	18.75 $\pm$ 6.11

**Table E8** The dimensionless parameters for PS/PP blends after shearing 5000 strain unit at the viscosity ratio of 3, 220 °C (Figure 4.15)

Polymer pairs	$\Gamma^*$ (dyn/cm)	$\gamma$ (s <sup>-1</sup> )	D ( $\mu$ m)	$\eta_d$ (Poise)	$\eta_m$ (Poise)	$\eta_r$	$N_{1,d}$ (dyn/cm <sup>2</sup> )	$N_{1,m}$ (dyn/cm <sup>2</sup> )	$N_{1,r}$	Ca
PS(1)/PP(2)	4.78	10	3.40 $\pm$ 0.93	2.82E+04	9.38E+03	3.01	3.86E+05	1.66E+05	2.33	6.38 $\pm$ 1.74
PS(1)/PP(3)	4.78	100	3.10 $\pm$ 0.74	5.24E+03	1.71E+03	3.06	9.83E+05	2.83E+05	3.47	10.66 $\pm$ 2.53
PS(1)/PP(4)	4.78	30	4.53 $\pm$ 1.03	1.35E+04	4.55E+03	2.97	8.29E+05	1.66E+05	4.99	12.37 $\pm$ 2.81
PS(1)/PP(4)	4.78	20	5.24 $\pm$ 1.04	1.81E+04	6.08E+03	2.97	6.56E+05	1.27E+05	5.17	12.75 $\pm$ 2.54

**Table F1** The shear viscosity ratio at pre-shearing of PS/PP blends, 220 °C

$\dot{\gamma}$ (s <sup>-1</sup> )	PS(1)/ PP(1)	PS(1)/ PP(2)	PS(1)/ PP(3)	PS(1)/ PP(4)	PS(2)/ PP(1)	PS(2)/ PP(2)	PS(2)/ PP(3)	PS(2)/ PP(4)	PS(3)/ PP(1)	PS(3)/ PP(2)	PS(3)/ PP(3)	PS(3)/ PP(4)
10	1.592	2.533	1.989	4.050	0.384	0.611	0.480	0.977	0.288	0.458	0.359	0.732
20	1.190	2.877	1.660	3.123	0.340	0.822	0.474	0.850	0.268	0.649	0.374	0.670
30	1.503	3.314	1.897	3.194	0.473	1.043	0.597	0.935	0.386	0.793	0.530	0.763
50	1.535	4.826	1.717	3.345	0.533	1.677	0.597	0.981	0.474	1.491	0.531	1.053
70	2.125	5.309	2.413	4.790	0.722	1.803	0.820	1.627	0.696	1.740	0.791	1.570
100	2.572	5.738	3.009	5.142	0.859	1.917	1.005	1.718	0.977	2.179	1.143	1.952

**Table F2** The first normal stress difference ratio at pre-shearing of PS/PP blends, 220 °C

$\dot{\gamma}$ (s <sup>-1</sup> )	PS(1)/ PP(1)	PS(1)/ PP(2)	PS(1)/ PP(3)	PS(1)/ PP(4)	PS(2)/ PP(1)	PS(2)/ PP(2)	PS(2)/ PP(3)	PS(2)/ PP(4)	PS(3)/ PP(1)	PS(3)/ PP(2)	PS(3)/ PP(3)	PS(3)/ PP(4)
10	1.760	1.404	2.573	6.498	0.238	0.315	0.368	0.878	0.155	0.205	0.226	0.571
20	1.626	2.387	2.105	4.313	0.313	0.409	0.405	0.830	0.213	0.312	0.275	0.564
30	1.575	2.341	1.559	3.389	0.417	0.529	0.446	0.898	0.300	0.346	0.341	0.646
50	1.342	2.309	1.684	2.656	0.552	0.938	0.595	1.115	0.406	0.699	0.492	0.924
70	1.171	2.338	1.505	2.538	0.542	1.081	0.696	1.174	0.452	0.903	0.581	0.980
100	1.218	2.027	2.334	2.185	0.582	0.969	0.667	1.044	0.646	1.075	0.687	1.159

**Table F3** The shear viscosity ratio after shearing 5000 strain unit of PS/PP blends, 220 °C

$\dot{\gamma}$ (s <sup>-1</sup> )	PS(1)/ PP(1)	PS(1)/ PP(2)	PS(1)/ PP(3)	PS(1)/ PP(4)	PS(2)/ PP(1)	PS(2)/ PP(2)	PS(2)/ PP(3)	PS(2)/ PP(4)	PS(3)/ PP(1)	PS(3)/ PP(2)	PS(3)/ PP(3)	PS(3)/ PP(4)
10	1.635	3.011	2.157	4.050	0.394	0.726	0.520	0.977	0.295	0.544	0.390	0.732
20	1.312	3.538	1.766	2.974	0.375	1.011	0.505	0.850	0.296	0.798	0.398	0.670
30	1.408	3.695	1.965	2.970	0.443	1.163	0.618	0.935	0.361	0.949	0.505	0.763
50	1.423	5.506	1.752	3.345	0.495	1.913	0.609	1.162	0.440	1.701	0.541	1.033
70	1.667	6.924	1.955	4.790	0.566	2.351	0.664	1.627	0.546	2.270	0.641	1.570
100	1.913	7.327	3.057	5.142	0.639	2.447	1.021	1.718	0.726	2.782	1.161	1.952

**Table F4** The first normal stress difference ratio after shearing 5000 strain unit of PS/PP blends, 220 °C

$\dot{\gamma}$ (s <sup>-1</sup> )	PS(1)/ PP(1)	PS(1)/ PP(2)	PS(1)/ PP(3)	PS(1)/ PP(4)	PS(2)/ PP(1)	PS(2)/ PP(2)	PS(2)/ PP(3)	PS(2)/ PP(4)	PS(3)/ PP(1)	PS(3)/ PP(2)	PS(3)/ PP(3)	PS(3)/ PP(4)
10	1.760	2.327	2.573	6.498	0.238	0.315	0.348	0.878	0.155	0.205	0.226	0.571
20	1.948	2.859	2.521	5.166	0.313	0.459	0.405	0.830	0.213	0.312	0.275	0.564
30	2.320	3.448	2.480	4.992	0.417	0.620	0.446	0.898	0.300	0.446	0.321	0.646
50	2.544	4.378	2.957	5.037	0.512	0.881	0.595	1.014	0.406	0.699	0.472	0.804
70	2.654	5.298	3.412	5.752	0.542	1.081	0.696	1.174	0.452	0.903	0.581	0.980
100	3.030	5.045	3.473	5.438	0.582	0.969	0.667	1.044	0.646	1.075	0.740	1.159

ต้นฉบับ หน้าขาดหาย

## **CURRICULUM VITAE**

**Name :** Ms. Chatriya Suamsung

**Birthday :** May 5, 1975

**Nationality :** Thai

**University Education :**

1993-1997 Bachelor's Degree of Chemistry  
King Mongkut's University of Technology  
Thonburi, Bangkok